The Journal of Chemical Physics

RAPID COMMUNICATION | FEBRUARY 04 2025

Resonance-enhanced multiphoton ionization detection of vibrationally excited O_2

Itai S. Kallos ; Kerim Benfreha ; Kai Golibrzuch ; Hao Zhao ; Ilana Bar ; Tim Schäfer ; Igor Rahinov ; Alec M. Wodtke ; Joshua H. Baraban

J. Chem. Phys. 162, 051103 (2025)
https://doi.org/10.1063/5.0251383

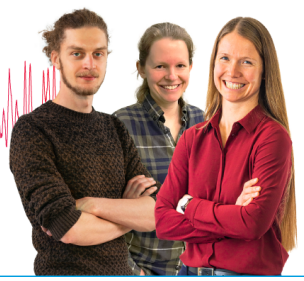

The Journal of Chemical Physics COMMUNICATION pubs.aip.org/aip/jcp

Resonance-enhanced multiphoton ionization detection of vibrationally excited O_2

Cite as: J. Chem. Phys. 162, 051103 (2025); doi: 10.1063/5.0251383
Submitted: 2 December 2024 • Accepted: 9 January 2025 •
Published Online: 4 February 2025

Itai S. Kallos,[1,2,3] Kerim Benfreha,[4] Kai Golibrzuch,[5] Hao Zhao,[6] Ilana Bar,[1] Tim Schäfer,[4] Igor Rahinov,[3] Alec M. Wodtke,[4,5] and Joshua H. Baraban[2,a)]

AFFILIATIONS

[1] Department of Physics, Ben-Gurion University of the Negev, Beer-Sheva 8410501, Israel
[2] Department of Chemistry, Ben-Gurion University of the Negev, Beer-Sheva 8410501, Israel
[3] Department of Natural Sciences, The Open University of Israel, 4353701 Raanana, Israel
[4] Institute for Physical Chemistry, Georg-August University of Goettingen, Tammannstraße 6, 37077 Goettingen, Germany
[5] Department of Dynamics at Surfaces, Max Planck Institute for Multidisciplinary Sciences, Am Fassberg 11, 37077 Goettingen, Germany
[6] College of Engineering, Peking University, Beijing 100871, People's Republic of China

[a)] **Author to whom correspondence should be addressed:** jbaraban@bgu.ac.il

ABSTRACT

We report a rotationally resolved spectroscopic detection scheme for vibrationally excited molecular oxygen with high sensitivity. Two-color $(2 + 1')$ resonance-enhanced multiphoton ionization (REMPI) spectra of O_2 hot bands were recorded for the first time via the $3d\pi\ (v' = 0) \leftarrow X\ ^3\Sigma_g^-\ (v'' = 1)$ Rydberg transitions. Spectroscopic constants and relative Franck–Condon factors were extracted and compared to simulations. This new access to quantum-state-resolved diagnostics of vibrationally excited O_2 promises to shed light on the physical and chemical dynamics of many processes.

I. INTRODUCTION

Molecular oxygen constitutes much of our atmosphere and the interstellar medium; its ubiquity and unique bi-radical nature lead to rich and prevalent physical and chemical dynamics. Although O_2 reacts exothermically with most compounds on Earth, activation barriers make most reaction rates negligible under ambient conditions. Electronically and vibrationally excited O_2 can often overcome these barriers, making it highly reactive; hence, excited O_2 plays a crucial role in many important and energetic processes spanning numerous fields. In combustion, hot O_2 is detected in combustor efficiency measurements[1] and can result in reduction of emissions;[2] in atmospheric chemistry, excited oxygen is produced via ultraviolet (UV) photolysis of ozone, affecting ozone recovery;[3–6] in plasma science, recombination of atomic oxygen, collisions, and high temperatures can vibrationally excite O_2;[7,8] and in surface chemistry, redox reactions and vibrational energy transfer at metal surfaces are of interest.[9,10] Despite the acute and extensive need for quantum-state-resolved information on O_2 to characterize its physical and chemical dynamics, suitable spectroscopic detection capabilities are not always available. A case in point concerns low-lying vibrational levels of the electronic ground state, which cannot be probed sensitively without vacuum ultraviolet (VUV) radiation. In this work, using our recently developed two-color $(2 + 1')$ ionization scheme,[11] we report the first observation of two-photon resonance-enhanced multiphoton ionization (REMPI) spectra of vibrationally excited O_2, acquired with rotational resolution via the $3d\pi$ Rydberg states.

Several methods have been utilized to detect hot molecular oxygen,[12] including Raman–Rayleigh scattering,[13–16] laser-induced fluorescence (LIF) by ~193, 202–228, ~225, and ~248 nm radiation,[17–24] coherent anti-Stokes Raman scattering (CARS),[25–27] and cavity ring-down spectroscopy (CRDS).[28] However, these methods suffer from one or more drawbacks, including insufficient sensitivity, use of VUV lasers to reach the Schumann–Runge bands,

spectral congestion due to many probed species, lack of fully rotationally resolved spectra, often due to the need to excite many rotational lines to achieve sufficient signal to noise ratio (SNR), and difficulties to directly probe non-equilibrium regions where radicals and other transient species drive complex chemistry.

REMPI is a highly sensitive spectroscopic method allowing for rovibrational specificity.[29] REMPI can also be augmented by other methods, notably time-of-flight mass-spectrometry (TOFMS) for mass selectivity,[30] microwave spectroscopy (Radar REMPI) for minimally invasive measurements,[31] temporal dynamics,[32] and recording temperatures,[33] and velocity map imaging[34] (VMI) allowing monitoring of velocity distributions. Combining VMI with rotationally resolved spectra in gas phase dynamics experiments provides complete information on the probed species' internal degrees of freedom.

Many one-color REMPI studies mapped the Rydberg states of O_2;[35–43] however, a REMPI spectrum of the vibrational hot bands of O_2 was never recorded. Even when hot O_2 in a flame was probed,[44] hot bands were not observed, likely due to spectral interferences and lack of sensitivity. Nevertheless, the recent development of two-color REMPI schemes has considerably improved sensitivity and versatility,[11] allowing us to record fully rotationally resolved spectra of the $3d\pi\ (v' = 0) \leftarrow X\ ^3\Sigma_g^-\ (v'' = 1)$ transitions. The results were compared to simulations, yielding band origins, spectroscopic constants, coupling constants, and relative Franck–Condon (FC) factors. This new access to quantum-resolved diagnostics of O_2 promises to shed light on many types of physical and chemical dynamics.

II. METHODS

This study was conducted on a previously described apparatus[45] with improved detection capabilities. A VMI setup similar to that previously described[46] was integrated into the TOFMS, allowing the measurement of velocity distributions. Ions are detected via multichannel plates (MCP, Topag MCP 56-15) found at the end of a 50 cm flight tube; a P43 phosphor screen (ProxiVision) is coupled to the MCP, allowing for visualization by using a complementary metal-oxide semiconductor (CMOS) camera (Basler ace acA1920-155 mm, 1920 × 1200 px). Supersonic expansion of oxygen helium mixture (1:9) at a backing pressure of 5 bar was produced using a home-built pulsed valve[47] with ~32 μs opening time and 10 Hz repetition rate. The gas was passed through a silicon carbide (SiC) tube (1 mm diameter, ~2 cm length) resistively heated up to 1000 K; the temperature was monitored via a K-type thermocouple and thermal camera (CT2MHCF IR-pyrometer). We note that we have since switched to a Series 9 pulsed valve and an alumina (Al_2O_3) tube heated by an insulated resistive wire.[48] Alumina does not oxidize like SiC, and this pulsed valve allows for the longer pulse durations needed to fill the tube during operation. These changes resulted in improved experimental conditions. The molecular beam (MB) passes through a 2 mm skimmer and a 2 mm aperture between differentially pumped chambers, reaching the interaction region, where pressure rises from $\sim 1 \times 10^{-9}$ to $\sim 1 \times 10^{-8}$ Torr. Ionization is performed by a recently developed two-color (2 + 1′) REMPI scheme[11] using a tunable frequency-doubled pulsed dye laser (Sirah, Cobra-Stretch, 2.5–3 mJ, ~0.04 cm^{-1} linewidth) pumped by a frequency-tripled Nd:YAG laser (Continuum, Surelite, SLXIII-EX) as the UV excitation source and a tunable fundamental pulsed dye laser (Sirah, Cobra-Stretch, 20–25 mJ, ~0.05 cm^{-1} linewidth) pumped by an additional frequency-doubled Nd:YAG laser (Spectra Physics, Quanta Ray Pro-230-10) as the visible (VIS) 744 nm ionization source. The lasers produce ~7.5 ns pulses at a 10 Hz repetition rate. The UV and VIS beams counter-propagate and are focused by 50 cm focal length plano-convex lenses; beams overlap spatially and temporally, and the densest MB section is chosen by controlling the pulsed valve and pump laser Q-switch delays via a delay generator (Stanford Research Systems, DG535). Detection of the REMPI signal is accomplished by the previously described VMI setup. The scanned laser wavelength is constantly monitored by coupling a reflection into a wavemeter (HighFinesse WS7), and excitation energy is monitored after the cell exit by a power meter (Gentec-EO Maestro).

III. RESULTS AND DISCUSSION

The (2 + 1′) REMPI spectra of excited O_2 was recorded for many of the $3d\pi\ (v' = 0) \leftarrow X\ ^3\Sigma_g^-\ (v'' = 0, 1)$ Rydberg transitions. The spectral region was chosen due to its high signal and the isolated nature of the v_1^0 bands, which do not overlap any ground state transitions. Thus, even a small amount of excited O_2 in cold-dominated oxygen mixtures can be detected, which is often an experimental prerequisite.[1] We note that v_0^0 and v_1^0 are found within the tuning range of a single dye, hence facilitating the determination of the (v_1^0/v_0^0) population ratio. Moreover, this scheme will presumably work for higher vibrationally excited states, for which v_2^0 and v_3^0 are also within the tuning range of the same dye. The v_1^0 spectral region was recorded using a pulsed valve and a SiC tube. The high temperature and nine observed electronic bands comprising the $3d\pi$ Rydberg complex[37] in the recorded spectral range result in a somewhat congested spectrum. For reliable assignments, additional scans of the $3d\pi\ v_0^0$ transitions were taken under different rotational cooling conditions: without a SiC tube (very cold), with a SiC tube (cold), and a SiC tube heated to 1000 K (hot); all four spectra can be seen in Fig. 1. The experimental spectra were normalized by UV laser power, which showed an almost quadratic dependence across all spectra, and fitted to PGOPHER[49] simulations to extract accurate rotational temperatures and spectroscopic constants. Colder spectra were used to assign bandheads, band origins, starting values for the rotational constants via combination differences, and spin–spin coupling constants. Rotational temperatures were extracted from the isolated $^1\Sigma_g^+(0)$ band (Fig. S1), resulting in ~5 K for the coldest spectrum. For spectra taken with the SiC tube, a bimodal temperature distribution was observed, likely due to insufficient gas flow to fully fill the tube and "choke" at the outlet, producing different mass flow elements in the final outlet pulse. Comparison with simulations showed 10, 25 K and 150, 500 K for the cold and hot simulations, respectively. The v_1^0 experimental and simulated spectral range including all observed electronic states can be seen in Fig. 2.

It is important to note that the band origins and B_v rotational constants derived from the very cold and cold spectra where the electronic bands are well separated significantly constrain the hotband simulation. This is because temperature influences the population, i.e., line intensities, but does not affect line positions. In addition, each electronic band has clear features and spacing (Fig. 2), which other bands cannot recreate without drastic changes to the

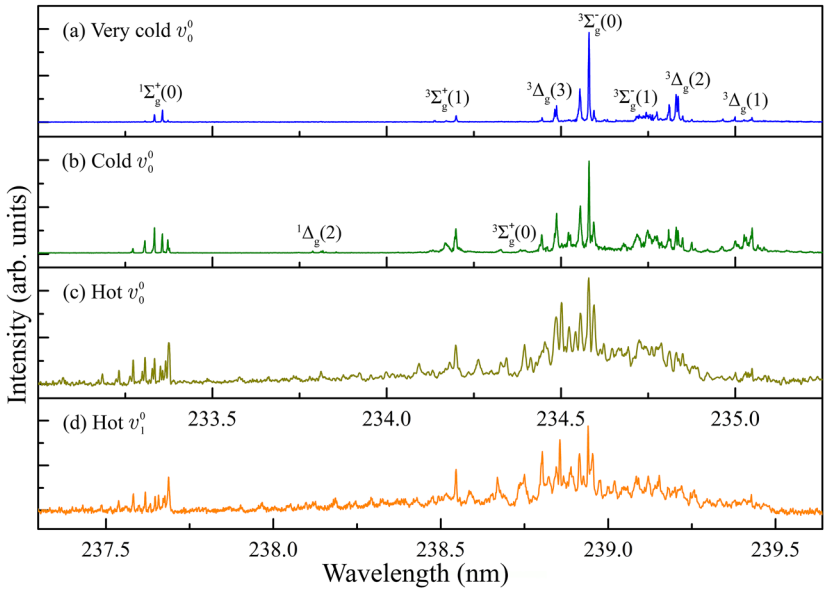

FIG. 1. Measured resonance-enhanced multiphoton ionization (REMPI) spectra of the $3d\pi(v' = 0) \leftarrow X\,^3\Sigma_g^-$ ($v'' = 0$, 1) Rydberg two-photon transitions of molecular oxygen at various rotational temperatures. The top three panels (a), (b), and (c) show the v_0^0 band spectra, with upper electronic states labeled, including spin–orbit terms in parentheses. The bottom panel (d) displays the v_1^0 hot band spectrum taken at the same temperature as the trace in panel c. Panel d is on a different wavelength range than the three v_0^0 panels, and the axis is slightly scaled for the bands to line up visually.

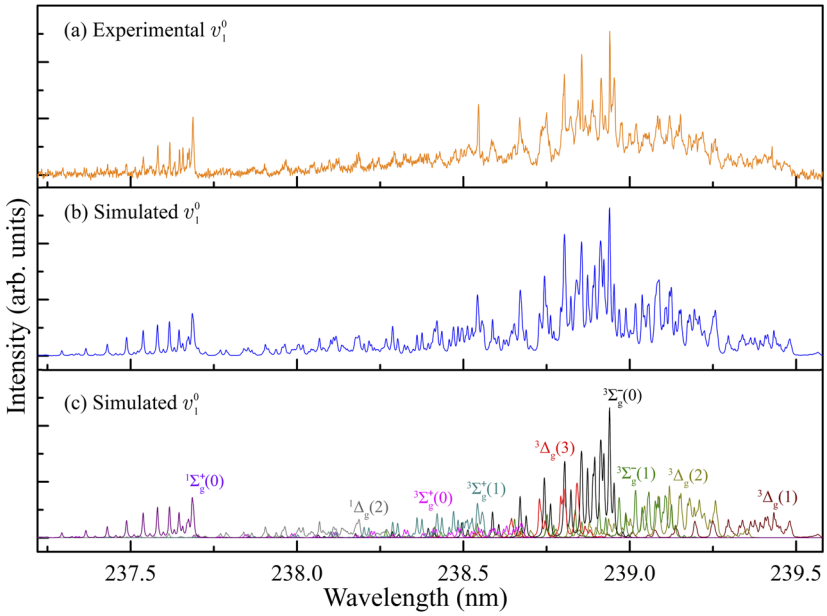

FIG. 2. Resonance-enhanced multiphoton ionization (REMPI) spectra of the $3d\pi(v' = 0) \leftarrow X\,^3\Sigma_g^-$ ($v'' = 1$) transitions of vibrationally excited molecular oxygen. The top panel (a) is an experimental REMPI spectrum of O_2 from the nozzle heated to 1000 K. The second panel (b) is a PGOPHER[49] simulation used to determine rotational temperature and constants, band origins, and coupling constants (Table I) with 0.001 and 0.0025 nm Lorentzian and Gaussian linewidths, respectively. The bottom panel (c) shows separately each of the nine electronic states that constitute the $3d\pi$ Rydberg complex in the recorded spectral range.

molecular constants. We note that the centrifugal distortion (CD) constants D_v and H_v were sometimes needed to adjust high J lines where definitive assignment is more challenging. Assignments for the $3d\pi(v' = 0) \leftarrow X\,^3\Sigma_g^-(v'' = 0)$ transitions via cold supersonic expansion of O_2 were previously performed;[37–41,50] band origins and rotational constants were assigned with a few exceptions.

Rotationally hot spectra of O_2 allowed us to refine known constants and determine additional parameters (Table I). Spectroscopic constants for the ground state were taken from Yu *et al.*[51] All bandheads were within several wavenumbers of those reported by Yokelson *et al.*[37] However, extracted rotational constants did not always agree, presumably due to the small number of J states visible in the cold literature spectra. Rotational constants are also compared to those tabulated by Ogorzalek Loo *et al.*[41] and Park *et al.*,[47] although only a few were reported. Spin–spin coupling constants ($\lambda_{s\text{-}s}$) were found empirically (Fig. S2). Their signs are consistent with the $^3\Sigma_g^-$ states lying energetically lower than $^3\Sigma_g^+$; while the opposite is expected from the $\pi\pi^*$ electronic configuration,[52] it has been shown that in this case, their order is reversed.[37] Relative FC factors were calculated (Table I) for each electronic state based on the v_1^0/v_0^0 PGOPHER simulation intensity integrals. The initial vibrational population is assumed as thermal, resulting in a ~9.6%

TABLE I. Rotational constants, origins, spin–spin couplings, and relative Franck–Condon factors for the $3d\pi$ ($v' = 0$) Rydberg states observed in this work. We estimate the uncertainty in the relative FC factors as ±0.5.

	$B_{v'=0}$ (cm^{-1})				$D_{v'=0}$ (cm^{-1})	$H_{v'=0}$ (cm^{-1})	Origin (cm^{-1})	$\lambda_{s\text{-}s}$ (cm^{-1})	(v_1^0/v_0^0) FC
State	37	39 and 50	41	This work	This work				
$^3\Sigma^-(0)$	1.850	⋯	1.745	1.94	1.0×10^{-5}	-9.0×10^{-8}	85 258	−4.5	5.6
$^3\Sigma^-(1)$	⋯	⋯	⋯	1.81	9.8×10^{-5}	⋯	85 194	−5.0	4.9
$^3\Sigma^+(0)$	⋯	⋯	⋯	1.94	-4.0×10^{-5}	⋯	85 357	2.1	4.5
$^3\Sigma^+(1)$	2.225	⋯	⋯	1.91	9.9×10^{-5}	⋯	85 400	2.9	6.3
$^1\Sigma^+(0)$	⋯	1.740	1.740	1.74	-5.0×10^{-7}	⋯	85 707	N/A	6.0
$^3\Delta(1)$	1.596	⋯	⋯	1.67	5.0×10^{-6}	⋯	85 079	0	10.3
$^3\Delta(2)$	1.585	⋯	⋯	1.62	1.0×10^{-5}	1.1×10^{-8}	85 158	0	4.8
$^3\Delta(3)$	1.675	⋯	⋯	2.14	⋯	⋯	85 284	0	4.5
$^1\Delta(2)$	⋯	1.813	1.760	1.65	⋯	⋯	85 535	N/A	5.5

Boltzmann population of the $v'' = 1$ level at a tube temperature of 1000 K. The high relative FC factors further strengthen our assumption that higher vibrational hot bands should be detectable even at low populations.

IV. CONCLUSIONS

REMPI spectra of vibrational hot bands of molecular oxygen were recorded for the first time using a newly developed two-color scheme via the $3d\pi$ Rydberg transitions. New spectroscopic constants were found and known constants refined. The advantages of REMPI and coupled techniques, notably mass spectrometry and VMI, result in a broad rotationally resolved spectral range, good SNR, mass selectivity, and velocity distribution. We expect these capabilities to aid state-selective studies of excited molecular oxygen dynamics in many physical and chemical fields.

SUPPLEMENTARY MATERIAL

See the supplementary material for additional data and discussion on the determination of temperature and spin–spin coupling constants.

ACKNOWLEDGMENTS

This project received funding from the European Research Council (ERC) under the European Union's Horizon 2020 research and innovation programme (Grant Agreement No. 848668), and the Israel Science Foundation under Grant No. 194/20. I.S.K. acknowledges support from a short-term BGU postdoctoral scholarship No. 434837, the Max Planck Society under the Israel MPI Partnership Program, an OUI Research Authority Grant No. 41838 (515651), and the Pazy Foundation under Grant Number 284-21. K.B., T.S., and A.M.W. acknowledge the support from the Sonderforschungsbereich 1633 under Project No. C02. T.S. acknowledges funding from the Deutsche Forschungsgemeinschaft under Grant No. SCHA 1946/5-1. H.Z. acknowledges support from the China National Petroleum Corporation-Peking University Strategic Cooperation Project of Fundamental Research.

AUTHOR DECLARATIONS

Conflict of Interest

I.S.K., I.B., and J.H.B. have Patent Application 63/726,270 pending.

Author Contributions

I.S.K. and K.B. contributed equally to this work.

Itai S. Kallos: Conceptualization (equal); Data curation (equal); Formal analysis (equal); Investigation (equal); Methodology (equal); Software (equal); Visualization (equal); Writing – original draft (lead); Writing – review & editing (equal). **Kerim Benfreha**: Data curation (equal); Investigation (equal); Methodology (equal). **Kai Golibrzuch**: Conceptualization (equal); Investigation (equal); Methodology (equal); Writing – review & editing (equal). **Hao Zhao**: Conceptualization (equal); Writing – review & editing (equal). **Ilana Bar**: Conceptualization (equal); Formal analysis (equal); Supervision (equal); Visualization (equal); Writing – review & editing (equal). **Tim Schäfer**: Conceptualization (equal); Data curation (equal); Formal analysis (equal); Funding acquisition (equal); Investigation (equal); Methodology (equal); Project administration (equal); Resources (equal); Supervision (equal); Validation (equal); Visualization (equal); Writing – review & editing (equal). **Igor Rahinov**: Conceptualization (equal); Formal analysis (equal); Funding acquisition (equal); Investigation (equal); Methodology (equal); Project administration (equal); Resources (equal); Supervision (equal); Visualization (equal); Writing – review & editing (equal). **Alec M. Wodtke**: Conceptualization (equal); Formal analysis (equal); Funding acquisition (equal); Investigation (equal); Methodology (equal); Project administration (equal); Resources (equal); Supervision (equal); Writing – review & editing (equal). **Joshua H. Baraban**: Conceptualization (equal); Formal analysis (equal); Funding acquisition (equal); Investigation (equal); Methodology (equal); Project administration (equal); Resources (equal); Supervision (equal); Visualization (equal); Writing – review & editing (equal).

DATA AVAILABILITY

The data that support the findings of this study are available from the corresponding author upon reasonable request.

REFERENCES

[1] N. Collings, J. A. Harris, and K. Glover, Meas. Sci. Technol. **24**, 095101 (2013).
[2] H. Nakamura, Y. Kuwayama, T. Onishi, T. Tezuka, S. Hasegawa, K. Maruta, T. Araake, and S. Mochida, Appl. Therm. Eng. **194**, 117077 (2021).
[3] R. L. Miller, A. G. Suits, P. L. Houston, R. Toumi, J. A. Mack, and A. M. Wodtke, Science **265**, 1831 (1994).
[4] Y. Matsumi and M. Kawasaki, Chem. Rev. **103**, 4767 (2003).
[5] T. G. Slanger and R. A. Copeland, Chem. Rev. **103**, 4731 (2003).
[6] V. N. Azyazov and M. C. Heaven, "Kinetics of active oxygen species with implications for atmospheric ozone chemistry," Int. J. Chem. Kinet. **47**, 93–103 (2015).
[7] N. L. Aleksandrov and E. M. Anokhin, J. Phys. D: Appl. Phys. **42**, 225210 (2009).
[8] K. Dittmann, K. Matyash, S. Nemschokmichal, J. Meichsner, and R. Schneider, Contrib. Plasma Phys. **50**, 942 (2010).
[9] I. Rahinov, A. Kandratsenka, T. Schäfer, P. Shirhatti, K. Golibrzuch, and A. M. Wodtke, Phys. Chem. Chem. Phys. **26**, 15090 (2024).
[10] D. N. Mueller, M. L. Machala, H. Bluhm, and W. C. Chueh, Nat. Commun. **6**, 6097 (2015).
[11] I. S. Kallos, I. Bar, and J. H. Baraban, J. Phys. Chem. Lett. **15**, 2639 (2024).
[12] A. R. Masri, R. W. Dibble, and R. S. Barlow, Prog. Energy Combust. Sci. **22**, 307 (1996).
[13] S. Lederman, Prog. Energy Combust. Sci. **3**, 1 (1977).
[14] A. C. Eckbreth, J. Quant. Spectrosc. Radiat. Transfer **40**, 369 (1988).
[15] P. A. Nooren, M. Versluis, T. H. van der Meer, R. S. Barlow, and J. H. Frank, Appl. Phys. B **71**, 95 (2000).
[16] M. C. Weikl, F. Beyrau, J. Kiefer, T. Seeger, and A. Leipertz, Opt. Lett. **31**, 1908 (2006).
[17] J. Kiefer, B. Zhou, J. Zetterberg, Z. Li, and M. Alden, Appl. Spectrosc. **68**, 1266 (2014).
[18] A. Cessou, P. Colin, and D. Stepowski, Symp. (Int.) Combust. **27**, 1039 (1998).
[19] G. Laufer, R. L. McKenzie, and D. G. Fletcher, Appl. Opt. **29**, 4873 (1990).
[20] M. P. Lee, P. H. Paul, and R. K. Hanson, Opt. Lett. **12**, 75 (1987).
[21] G. A. Massey and C. J. Lemon, IEEE J. Quantum Electron. **20**, 454 (1984).
[22] M. D. Di Rosa, K. G. Klavuhn, and K. H. Ronald, Combust. Sci. Technol. **118**, 257 (1996).
[23] R. B. Miles and W. R. Lempert, Annu. Rev. Mech. **29**, 285 (1997).
[24] J. E. M. Goldsmith and R. J. M. Anderson, Opt. Lett. **11**, 67 (1986).
[25] S. Roy, J. R. Gord, and A. K. Patnaik, Prog. Energy Combust. Sci. **36**, 280 (2010).
[26] T. Seeger, F. Beyrau, A. Bräuer, and A. Leipertz, J. Raman Spectrosc. **34**, 932 (2003).
[27] L. Martinsson, P.-E. Bengtsson, and M. Aldén, Appl. Phys. B **62**, 29 (1996).
[28] G. D. Stancu, F. Kaddouri, D. A. Lacoste, and C. O. Laux, J. Phys. D: Appl. Phys. **43**, 124002 (2010).
[29] D. M. Lubman and M. N. Kronick, Anal. Chem. **54**, 660 (1982).
[30] T. Streibel and R. Zimmermann, Annu. Rev. Anal. Chem. **7**, 361 (2014).
[31] Z. Zhang, M. N. Shneider, and R. B. Miles, Plasma Sources Sci. Technol. **30**, 103001 (2021).
[32] A. Shashurin, M. N. Shneider, A. Dogariu, R. B. Miles, and M. Keidar, Appl. Phys. Lett. **96**, 171502 (2010).
[33] R. B. Miles, J. B. Michael, C. M. Limbach, S. D. McGuire, T. L. Chng, M. R. Edwards, N. J. DeLuca, M. N. Shneider, and A. Dogariu, Philos. Trans. R. Soc., A **373**, 20140338 (2015).
[34] A. T. J. B. Eppink and D. H. Parker, Rev. Sci. Instrum. **68**, 3477 (1997).
[35] B. R. Lewis, S. T. Gibson, J. S. Morrill, and M. L. Ginter, J. Chem. Phys. **111**, 186 (1999).
[36] R. J. Yokelson, R. J. Lipert, and W. A. Chupka, J. Chem. Phys. **97**, 6144 (1992).
[37] R. J. Yokelson, R. J. Lipert, and W. A. Chupka, J. Chem. Phys. **97**, 6153 (1992).
[38] P. Haiyoon, P. J. Miller, W. A. Chupka, and S. D. Colson, J. Chem. Phys. **89**, 6676 (1988).
[39] P. Haiyoon, L. Leping, and W. A. Chupka, J. Chem. Phys. **92**, 61 (1990).
[40] P. Haiyoon, L. Leping, and W. A. Chupka, J. Chem. Phys. **92**, 5835 (1990).
[41] R. Ogorzalek Loo, W. J. Marinelli, P. L. Houston, S. Arepalli, J. R. Wiesenfeld, and R. W. Field, J. Chem. Phys. **91**, 5185 (1989).
[42] S. T. Pratt, J. L. Dehmer, and P. M. Dehmer, J. Chem. Phys. **93**, 3072 (1990).
[43] J. S. Morrill, M. L. Ginter, E. S. Hwang, T. G. Slanger, R. A. Copeland, B. R. Lewis, and S. T. Gibson, J. Mol. Spectrosc. **219**, 200 (2003).
[44] P. J. H. Tjossem and K. C. Smyth, Chem. Phys. Lett. **144**, 51 (1988).
[45] Q. Ran, D. Matsiev, A. M. Wodtke, and D. J. Auerbach, Rev. Sci. Instrum. **78**, 104104 (2007).
[46] A. C. Dorst, R. E. A. Dissanayake, D. Schauermann, S. Knies, A. M. Wodtke, D. R. Killelea, and T. Schäfer, Front. Chem. **11**, 1248456 (2023).
[47] G. B. Park, B. C. Krüger, S. Meyer, D. Schwarzer, and T. Schäfer, J. Chem. Phys. **144**, 194308 (2016).
[48] J. H. Baraban, D. E. David, G. B. Ellison, and J. W. Daily, Rev. Sci. Instrum. **87**, 014101 (2016).
[49] C. M. Western, J. Quant. Spectrosc. Radiat. Transfer **186**, 221 (2017).
[50] H. Park, L. Li, and W. A. Chupka, Chem. Phys. Lett. **162**, 317 (1989).
[51] S. Yu, B. J. Drouin, and C. E. Miller, J. Chem. Phys. **141**, 174302 (2014).
[52] H. Lefebvre-Brion and R. W. Field, *The Spectra and Dynamics of Diatomic Molecules* (Elsevier, 2004).